

Thermal-mechanical fatigue simulation of a P91 steel in a temperature range of 400-600°C

A.A. Saad^{1,2}, C.J. Hyde^{1*}, W. Sun¹ and T.H. Hyde¹

¹Department of Mechanical, Materials and Manufacturing Engineering,
University of Nottingham, NG7 2RD, UK

²School of Mechanical Engineering, Universiti Sains Malaysia,
14300 Nibong Tebal, Penang, Malaysia

* Corresponding author: Christopher.Hyde@nottingham.ac.uk

Abstract

This paper deals with the identification of material constants to simulate the effect of cyclic mechanical loading and temperatures. A Chaboche viscoplasticity model was used in this study to model the thermal-mechanical behaviour of a P91 martensitic steel. A fully-reversed cyclic mechanical testing programme was conducted isothermally between 400 and 600°C with a strain amplitude of 0.5%, to identify the model constants using a thermo-mechanical fatigue (TMF) test machine. Thermo-mechanical tests of P91 steel were conducted for two temperature ranges of 400 to 500°C and 400 to 600°C. From the test results, it can be seen that the P91 steel exhibits cyclic softening throughout the life of the specimens, for both isothermal and thermal-mechanical loading and this effect can be modelled by the set of viscoplasticity constants obtained. Finite element simulations of the test specimens show good comparison to isothermal and TMF experimental data.

Keywords: Thermo-mechanical fatigue; viscoplasticity model; P91 steel; FE prediction

1. Introduction

Having an understanding of the thermo-mechanical behaviour of power plant materials has become more important as the operation of power plant moves to cyclic operation instead of base load operation. The operation at high temperature also emphasizes the importance of the creep phenomenon, while the cyclic loads introduce the fatigue phenomenon into the considerations. For instance, thermal fatigue loading may cause bore cracking due to the effects of varying steam temperature [1]. Severe thermal gradients between the inside and outside of components can cause high stress levels to develop.

The majority of studies on power plant materials have been related to the creep behaviour under constant load operation. For example, creep constitutive equations have been developed for the parent, heat-affected zone (HAZ) and weld materials of Cr-Mo-V steel welds in the range 565-640°C [2]. Similar studies have been carried out, for a P91 steel, in order to develop a creep constitutive model with a damage capability [3]. The development of these creep constitutive models have contributed to the gaining of a better understanding of the material behaviour in such applications as welding process modelling [4] and failure prediction in multiaxial components [5].

In contrast to the above applications, creep constitutive models which deal with cyclic loading conditions have had relatively little attention. Thus, a model which can include both cyclic and viscous effects is required. A commonly used model is the viscoplasticity model originally developed by Chaboche [6]. This viscoplasticity model has been used in many researches, including aeroengine materials such as nickel-based alloys [7]. However, the viscoplasticity model is rarely used to represent the behaviour of power plant materials. Research carried out on martensitic hot worked tool steels, which exhibits cyclic softening behaviour, has been used to develop an alternative type of viscoplasticity model [8].

The aim of the present study is to develop a constitutive model, particularly a viscoplasticity model, which can simulate the mechanical behaviour of power plant material under thermo-mechanical fatigue conditions. Isothermal strain-controlled tests have been performed on parent material of a pipe section to characterize the material behaviour, and a set of constants were determined from the test

data. Also, a series of thermo-mechanical fatigue tests were carried out between 400 and 600°C. The material constants were implemented in finite-element software to simulate the behaviour under isothermal and TMF conditions, using an axisymmetric model.

2. Experimental procedures

2.1 Material and test equipment

A martensitic P91 steel was used for the tests; specimens were machined from the parent material of a P91 pipe section. The chemical compositions of the material are given in Table 1. Figure 1 shows the dimensions of the cylindrical specimens used for all of the tests. The gauge sections of the specimens are 15mm in length and 6.5mm in diameter; these were finished by fine turning and polishing to a roughness average value of 0.8µm.

Table 1: Chemical compositions of the P91 steel (wt%).

Cr	Mo	C	Si	S	P	Al	V	Nb	N	W
8.60	1.02	0.12	0.34	<0.002	0.017	0.007	0.24	0.070	0.060	0.03

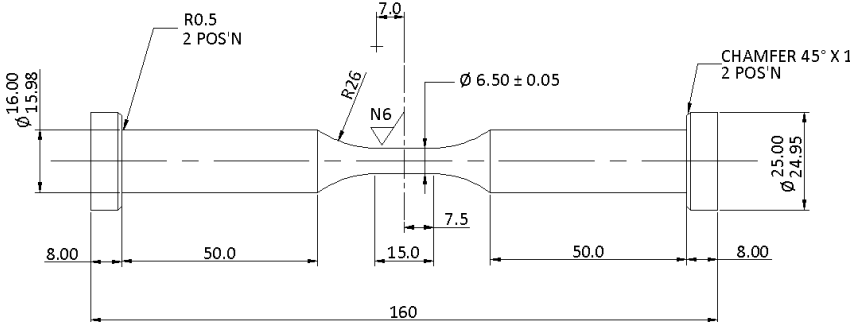


Figure 1: The specimen geometry used in the experiment.

All experiments were performed using an Instron 8862 TMF system, which utilizes radio-frequency induction heating, as shown in Figure 2. The coil design enables the temperature along the gauge section to be controlled to within ±10°C of the target temperature. The maximum achievable load for the machine is 35kN. The machine is controlled by a servo electric screw driven actuator. Strains were measured using a high temperature extensometer with a reference length of 12.5mm.

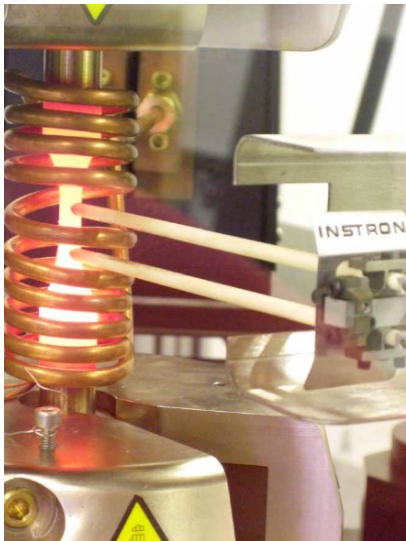


Figure 2: The Instron 8862 TMF machine system used for the tests.

2.2 Isothermal and TMF tests

Fully-reversed isothermal tests were conducted at 400, 500 and 600°C by controlling the total strain at a constant strain amplitude of $\pm 0.5\%$. Two specimens were tested at each temperature; one with continuous strain cycling and the other with a tension strain hold. A strain rate of 0.1%/s was used for all tests, which results in a cyclic period of 20s for the continuous strain cycling tests. For the tension strain hold test, the strain was held constant at peak tensile strain for 2 minutes. All tests were carried out to failure and stress-strain data for these tests were used in generating the viscoplasticity model.

The thermo-mechanical fatigue tests were implemented by controlling mechanical strain and temperature ranges. A mechanical strain range of $\pm 0.5\%$ was used for all of the thermo-mechanical fatigue tests. The machine controls the total strain value by automatically including the thermal strain for temperature ranges of 400 to 500°C or 400 to 600°C, as measured during initial tests prior to the actual TMF tests. The temperatures and strains were cycled under in-phase loading conditions (maximum temperature at maximum strain) up to failure; these TMF tests were repeated with a new specimen for the same temperature range with out-of-phase loading conditions (minimum temperature at maximum strain). All of the TMF tests were carried out with a period of 60s per cycle.

3. Material model characterization

3.1 The material model

The Chaboche unified viscoplasticity model [6] was chosen to model the behaviour of the P91 steel, under thermo-mechanical conditions. For the anisothermal conditions, total strain, ϵ , can be decomposed into elastic, ϵ_e , viscoplastic, ϵ_p , and thermal, ϵ_{th} , strain components as follows:

$$\epsilon = \epsilon_e + \epsilon_p + \epsilon_{th} \quad (1)$$

The viscoplastic strain rate, $\dot{\epsilon}_p$, and the yield criterion, f , are given by

$$\dot{\epsilon}_p = \left\langle \frac{f}{Z} \right\rangle^n \text{sgn}(\sigma - \chi) \quad (2)$$

$$f = |\sigma - \chi| - R - k \quad (3)$$

where Z and n are material constants, σ is the applied stress, k is the initial cyclic yield stress, χ is the kinematic hardening parameter and R is the isotropic hardening parameter. Also,

$$\text{sgn}(x) = \begin{cases} 1, & x > 0 \\ 0, & x = 0 \\ -1, & x < 0 \end{cases} \quad \text{and} \quad \langle x \rangle = \begin{cases} x, & x > 0 \\ 0, & x \leq 0 \end{cases}$$

The kinematic and isotropic hardening behaviours are described by the following equations

$$\dot{\chi}_i = C_i (a_i \dot{\epsilon}_p - \chi_i \dot{p}) \quad (4)$$

$$\chi = \chi_1 + \chi_2 \quad (5)$$

$$\dot{R} = b(Q - R)\dot{p} \quad (6)$$

where $i = 1, 2$; p is the accumulative viscoplastic strain; a_i and C_i represent the stationary values of χ_i and the speed to reach the stationary values, respectively, and Q is the asymptotic value of the isotropic variable, R , at stabilized cyclic condition and b governs the stabilization speed.

Generally, isotropic and kinematic hardening behaviours represent an expansion and a translation of the yield surface, respectively. For the viscoplasticity model, the load point may lie outside the yield surface [9] and this specific behaviour for the model is represented by viscous stress, σ_v , as follows

$$\sigma_v = Z\dot{p}^{1/n} \quad (7)$$

Thus, the applied stress can be decomposed as

$$\sigma = \chi + (R + k + \sigma_v) \text{sgn}(\sigma - \chi) = E(\epsilon - \epsilon_p) \quad (8)$$

The equations mentioned above are in uniaxial forms which will be used in the next section for material constant determination using the strain-controlled test data at 400, 500 and 600°C.

3.2 Identification of the viscoplasticity model constants

All of the viscoplasticity constants in this study were determined using the isothermal experimental results. From the data, 10 material constants need to be identified based on the equations given above and this section will explain briefly the process used for constants identification. Detailed explanations can be found in references [10] and [11].

Young's modulus, E , was identified from the slope of linear region for the first quarter cycle of the experiment, as shown in Figure 3. Generally, the first point to deviate from linear region is considered to be the yield stress. For instance, the stress at that point for P91 steel at 600°C, as shown in Figure 3, is around 200MPa. However, the results of uniaxial creep tests on the same material, tested at 600°C with 140 MPa stress level, produced creep straining and failed at 1454 hours. This condition shows that inelastic strain, or known as viscoplastic strain in this model, occurs at stress level lower than the conventional yield stress. In this study, the initial cyclic yield stress, k , value was estimated [10] as shown in Figure 3.

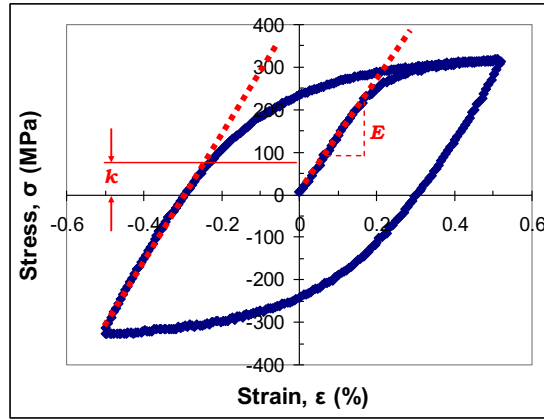


Figure 3: Example plots for obtaining Young's modulus, E , and estimation of initial cyclic yield stress, k , for P91 at 600°C.

All of the P91 test results produced cyclic softening, i.e. the stress ranges decrease in a strain-controlled condition. Normally, parameters Q and b are determined by using stress values from the stabilized period. However, before the stabilized period occurs, in the P91 tests, the material continued to cyclically soften due to material damage, as shown by the test data in Figure 4. Thus, the stabilized period was taken to be that at the half of life cycles. Equation (6) can be integrated to give the evolution of isotropic softening as

$$R = Q(1 - e^{-bp}) \quad (9)$$

The constant Q was taken to be the stress difference between the first and stabilized cycles, which gives a negative value for Q . The parameter p is approximately two times the plastic strain range data for each cycle and its value accumulates as cycles increase. Then, constant b was determined by fitting equation (9) to the test data as shown in Figure 4.

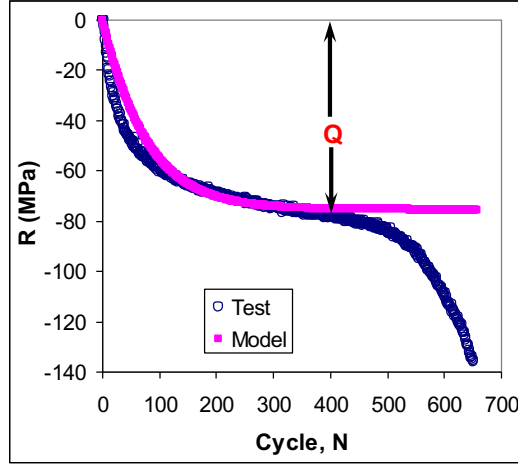


Figure 4: Cyclic softening and determination of b and Q at 600°C .

Kinematic hardening constants a_1 , C_1 , a_2 and C_2 were determined using the first-quarter of the tensile curve from the strain-controlled tests. The hardening data were generally divided into two regions to represent firstly the transient region of the inelastic deformation and secondly the region with greater inelastic strain [12]. Equation (4) can be integrated with respect to time to give the following equations:

$$\chi_1 = a_1(1 - e^{-C_1\varepsilon_p}) \quad (10)$$

$$\chi_2 = a_2(1 - e^{-C_2\varepsilon_p}) \quad (11)$$

Equations (10) and (11) can be substituted into equation (8). Differentiating Equation (8), with respect to ε_p , by assuming that χ_1 has a negligible effect on the hardening of χ_2 , gives

$$\frac{\partial\sigma}{\partial\varepsilon_p} - \frac{\partial R}{\partial\varepsilon_p} = a_2 C_2 e^{-C_2\varepsilon_p} \quad (12)$$

Thus, plotting $\ln[(\partial\sigma/\partial\varepsilon_p) - (\partial R/\partial\varepsilon_p)]$ versus ε_p , as shown in Figure 5, allows the identification of C_2 from the gradient and a_2 from the y-axis intercept. Similarly, a_1 and C_1 can be found for the lower strain region by plotting $\ln[(\partial\sigma/\partial\varepsilon_p) - (\partial R/\partial\varepsilon_p) - (\partial\chi_2/\partial\varepsilon_p)]$ versus ε_p [10].

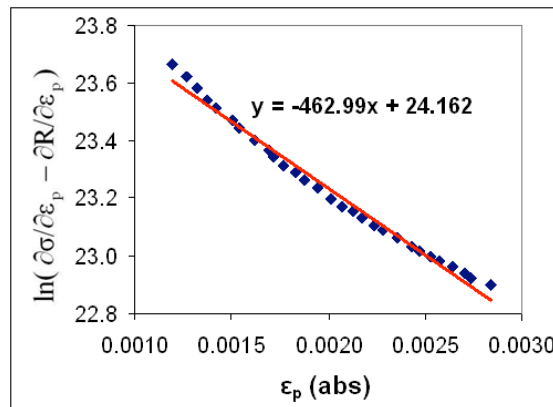


Figure 5: Kinematic hardening constant determination at 600°C .

By using the 8 constants identified so far, spreadsheet calculations for the viscoplasticity equations were implemented and constants Z and n were modified to obtain good fits to stress relaxation test data, as shown in Figure 6. All of the P91 material constants, determined using isothermal test data, are presented in Table 2.

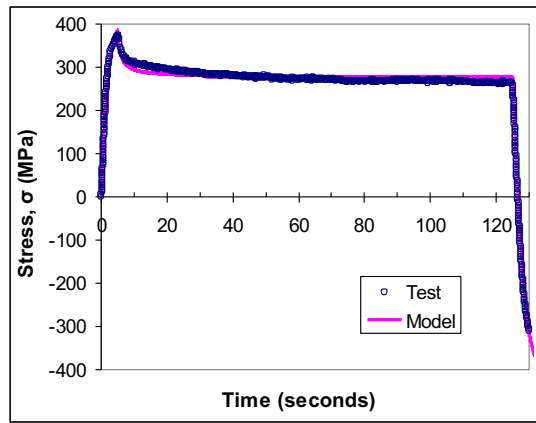


Figure 6: Fitting of Z and n constants to give best-fit to stress relaxation data for the first cycle, at 500°C.

Table 2: The material constants for the viscoplasticity model of P91 steel.

Temp. (°C)	E (MPa)	k (MPa)	Q (MPa)	b	a ₁ (MPa)	C ₁	a ₂ (MPa)	C ₂	Z (MPa.s ^{1/n})	n
400	187537.0	96	-55.0	0.45	150.0	2350.0	120.0	405.0	2000	2.25
500	181321.6	90	-60.0	0.6	98.5	2191.6	104.7	460.7	1875	2.55
600	139395.2	85	-75.4	1.0	52.0	2055.0	67.3	463.0	1750	2.7

4. Comparison of test and simulation results and discussions

Finite element simulation of isothermal and TMF conditions were implemented using an axisymmetric model in ABAQUS software. The model was based on the gauge section of cylindrical specimen with a diameter of 6.5mm and a gauge length of 12.5mm. Displacement control was applied in order to get the same strain range as that for the experimental data. For anisothermal conditions, temperature was applied for the whole geometry and a coefficient of thermal expansion of $14.5 \times 10^{-6}/^{\circ}\text{C}$, which is determined from TMF test results, was applied to include the effect of thermal strain in TMF tests. The constants in Table 2 were used to represent the viscoplastic behaviour of P91 between 400 and 600°C.

Figure 7, 8 and 9 compare the results of axisymmetric finite element simulations with the isothermal experimental data at 400, 500 and 600°C, respectively. The results at around half-life at each temperature are represented by Figure 7(b), 8(b) and 9(b). From these figures, simulation results are found to be in good agreement with the experimental data even though all the constants (except Q and b) were determined from the experimental data for the first cycle. This indicates that the model will give good predictions of thermo-mechanical behaviour between 400 and 600°C.

The viscoplasticity model successfully simulates cyclic softening behaviour by using a negative value for the constant Q. As shown by Figures 7, 8 and 9, reductions of stress, particularly the maximum stress level, are represented well at half-life cycles at each temperature. However, the cyclic softening effect of the model is valid only for cycles around the half-life to failure. The softening behaviour, at the end of life cycles, may be related to material damage which the current material model does not include.

The comparison results of thermo-mechanical simulations and experimental results are shown in Figure 10, 11, 12 and 13 and the simulation results are generally in good agreement with experimental data. These figures also show that the P91 steel softens cyclically under TMF conditions as indicated by the stress range reduction with cycle number. Figure 11, which present the results at 400-600°C with an out-of-phase condition, gives 100MPa peak stress difference in compression. However, the cyclic trends of this figure are similar where the stress levels become stable between 500 and 600°C in compressive strain. Similarly, Figure 10 also shows a similar trend for steady stress levels at temperature between 500 and 600°C. Even though the specimen corresponding to this figure (Figure 10) failed after a very small number of cycles (less than 10 cycles), the stress-strain data are still

important in order to show the significance of the creep between 500 and 600°C. For this TMF experimental data presented, it can be seen that there is some instability (i.e. data is not as smooth as other data) when compared to the isothermal equivalents. This is due to the instability of the air cooling through the centre of the specimen due to an ambitious waveform being used (i.e. small time period per cycle and therefore sudden, rapid heating/cooling which results heating/cooling ‘blasts’). Subsequently, it has been found that this effect can be reduced by constantly applying a small amount of cooling air through the centre of the specimen (~5%) during all regions of the waveform, including the heating of the specimen. This means that when an increase in air cooling is required, it can ramp up in a much more controlled manner.

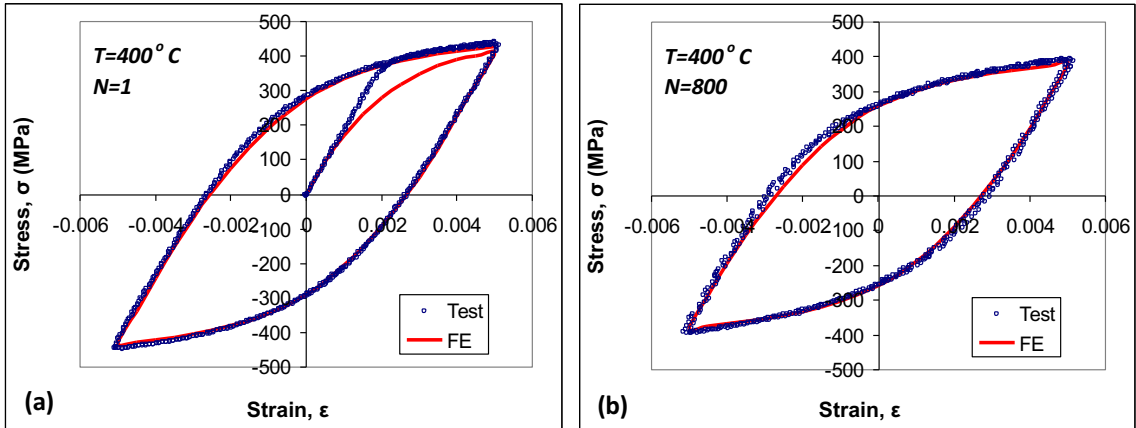


Figure 7: Comparison of FE simulation results with experimental data at 400°C for (a) first cycle and (b) 800 cycles.

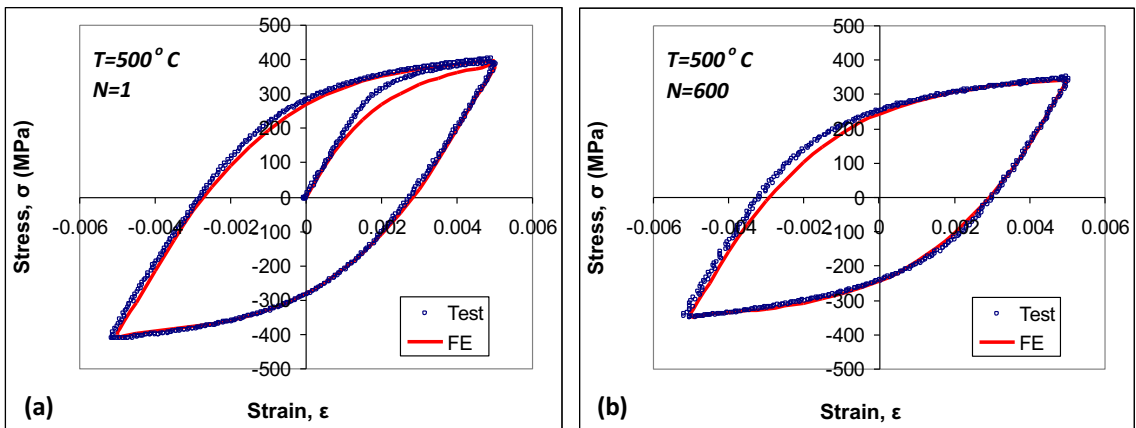


Figure 8: Comparison of FE simulation results with experimental data at 500°C for (a) first cycle and (b) 600 cycles.

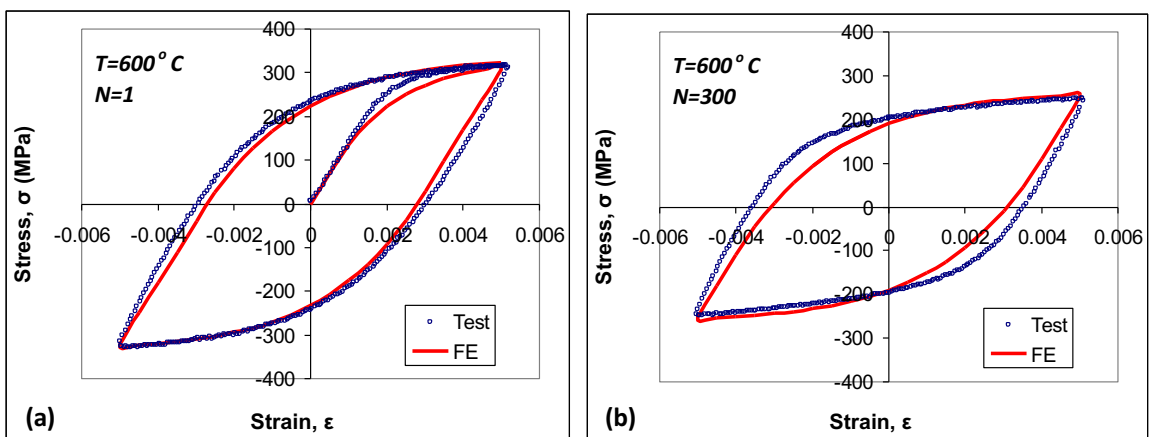


Figure 9: Comparison of FE simulation results with experimental data at 600°C for (a) first cycle and (b) 300 cycles.

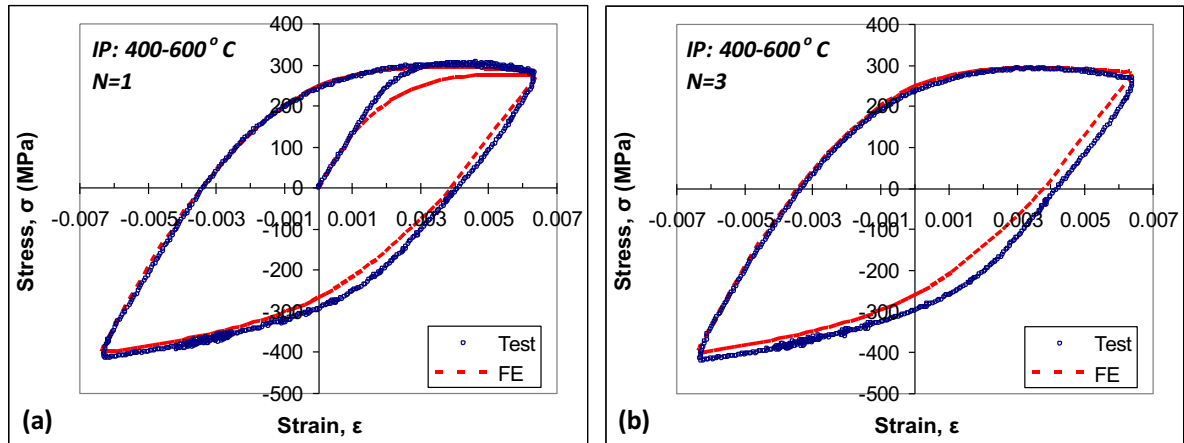


Figure 10: Comparison of FE simulation results with experimental data for an in-phase TMF condition, with a temperature range of 400-600°C at (a) first cycle and (b) 3 cycles.

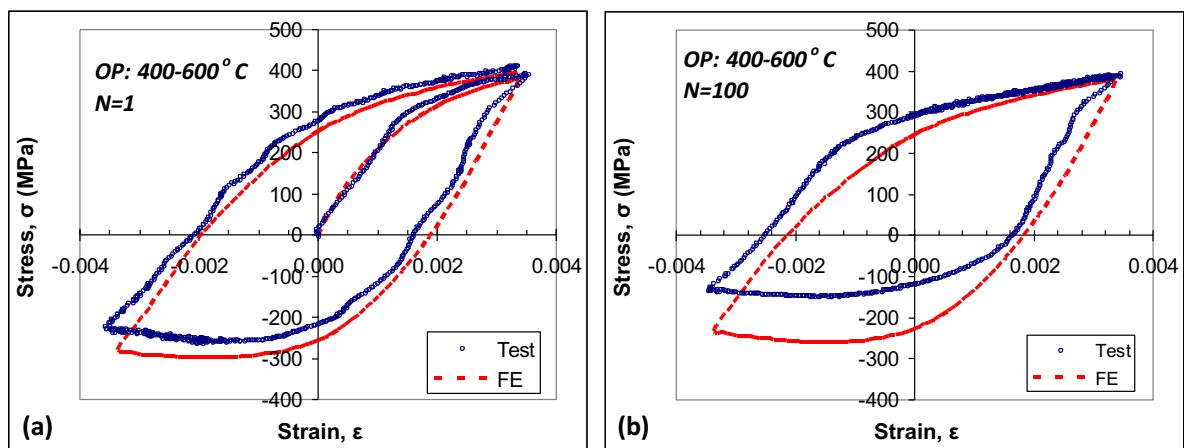


Figure 11: Comparison of FE simulation results with experimental data for an out-phase TMF condition, with a temperature range of 400-600°C at (a) first cycle and (b) 100 cycles.

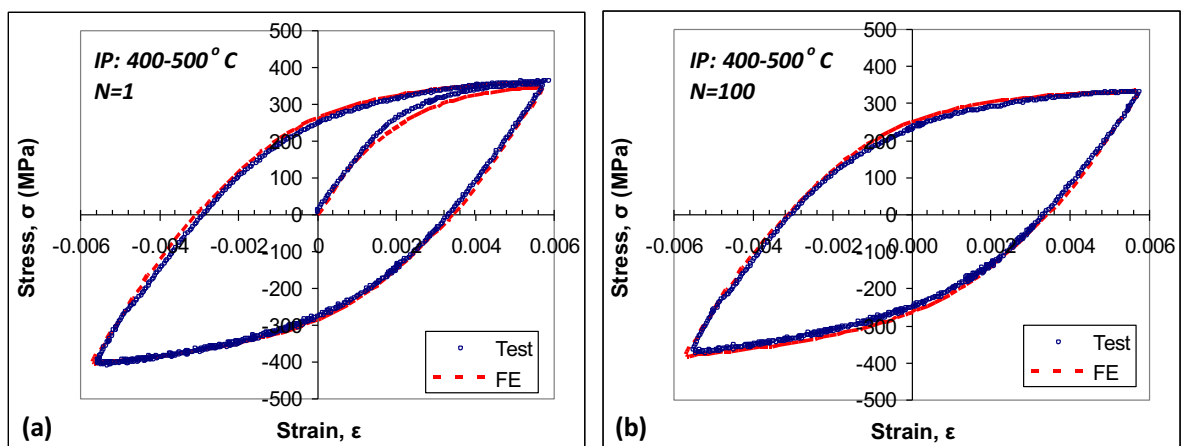


Figure 12: Comparison of FE simulation results with experimental data for an in-phase TMF condition, with a temperature range of 400-500°C at (a) first cycle and (b) 100 cycles.

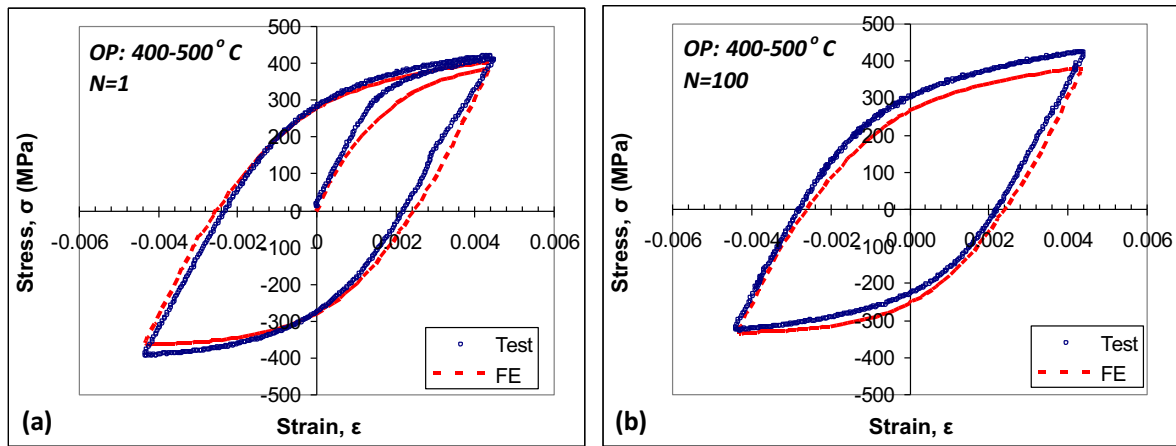


Figure 13: Comparison of FE simulation results with experimental data for an out-phase TMF condition, with a temperature range of 400-500°C at (a) first cycle and (b) 100 cycles.

5. Conclusions and future work

The P91 steel behaviour was investigated between temperature range within 400 to 600°C and a set of viscoplasticity model constants was obtained. Several conclusions can be drawn from this study, as follows:

- identification of viscoplasticity constants using data from the isothermal tests gives good comparison to thermo-mechanical behaviour between 400 and 600°C;
- cyclic softening of P91 steel can be represented by the viscoplasticity model by using a negative value for the constant Q ;
- the initial yield stress of the material used in the viscoplasticity model, particularly at elevated temperature, is lower than the yield stress value obtained from a conventional tensile test; and
- creep effects are significant for P91 steel in the temperature range between 500 and 600°C.

The current viscoplasticity constants will be further improved by using an optimization method, in order to get a more accurate fit to the experimental data. Further work is needed in order to include the time-dependency effect at elevated temperature and to improve the model performance, in order to establish a lifing model for failure cycle prediction.

6. Acknowledgements

We would like to acknowledge the support of EPSRC through the Supergen 2 programme (GR/S86334/01 and EP/F029748) and the following companies: Alstom Power Ltd., Tata Steel, E.ON Engineering Ltd., Doosan Babcock Energy Ltd., National Physical Laboratory, QinetiQ, Rolls-Royce plc, RWE npower, Sermatech Ltd. and Siemens Industrial Turbomachinery Ltd. for their valuable contributions to the project. C. J. Hyde would like to thank the EPSRC and the University of Nottingham for the funding through a Doctoral Training Programme and a PhD Plus scheme. The authors would also like to thank Tom Buss at the University of Nottingham for his assistance with the experimental work.

7. References

1. Brett SJ. Service experience of weld cracking in CrMoV steam pipework systems. *2nd International Conference on Integrity of High Temperature Welds*. London, 2003, pp. 3-17.
2. Hayhurst RJ, Mustata R, Hayhurst DR. Creep constitutive equations for parent, Type IV, R-HAZ, CG-HAZ and weld material in the range 565-640 °C for Cr-Mo-V weldments. *International Journal of Pressure Vessels and Piping*, 2005; **82**(2):137-144.
3. Hyde TH, Becker AA, Sun W, Williams JA. Finite-element creep damage analyses of P91 pipes. *International Journal of Pressure Vessels and Piping*, 2006; **83**(11-12): 853-863.
4. Yaghi AH, Hyde TH, Becker AA, Sun W. Finite element simulation of welding and residual stresses in a P91 steel pipe incorporating solid-state phase transformation and post-weld heat treatment. *Journal of Strain Analysis for Engineering Design*, 2008; **43**(5): 275-293.

5. Hayhurst DR, Lin J, Hayhurst RJ. Failure in notched tension bars due to high-temperature creep: Interaction between nucleation controlled cavity growth and continuum cavity growth. *International Journal of Solids and Structures*, 2008; **45**(7-8): 2233-2250.
6. Chaboche JL, Rousselier G. On the plastic and viscoplastic constitutive equations - Part 1: Rules developed with internal variable concept. *Journal of Pressure Vessel Technology*, 1983; **105**: 153-159.
7. Yaguchi M, Yamamoto M, Ogata T. A viscoplastic constitutive model for nickel-base superalloy, part 1: kinematic hardening rule of anisotropic dynamic recovery. *International Journal of Plasticity*, 2002; **18**(8): 1083-1109.
8. Zhang Z, Delagnes D, Bernhart G. Anisothermal cyclic plasticity modelling of martensitic steels. *International Journal of Fatigue*, 2002 ;**24**(6): 635-648.
9. Dunne F, Petrinic N. Introduction to Computational Plasticity. Oxford: Oxford University Press, 2007.
10. Zhan Z. A study of creep-fatigue interaction in a new nickel-based superalloy. University of Portsmouth, 2004.
11. Hyde CJ, Sun W, Leen SB. Cyclic thermo-mechanical material modelling and testing of 316 stainless steel. *International Journal of Pressure Vessels and Piping*, 2010; **87**(6): 365-372.
12. Tong J, Zhan ZL, Vermeulen B. Modelling of cyclic plasticity and viscoplasticity of a nickel-based alloy using Chaboche constitutive equations. *International Journal of Fatigue*, 2004 ;**26**(8): 829-837.